

# Determination of the interstitial electron density in liquid metals: Basic quantity to calculate the ion collective-mode velocity and related properties

L. Sani,<sup>1</sup> C. Petrillo,<sup>1,2</sup> and F. Sacchetti<sup>1,2</sup><sup>1</sup>*Dipartimento di Fisica, Università di Perugia, Via Alessandro Pascoli, I-06123 Perugia, Italy*<sup>2</sup>*Istituto Officina dei Materiali del Consiglio Nazionale delle Ricerche, Unità di Perugia, c/o Dipartimento di Fisica, Università di Perugia, Via Alessandro Pascoli, I-06123 Perugia, Italy*

(Received 19 August 2013; revised manuscript received 10 July 2014; published 31 July 2014)

Considering that various investigations identified a correlation between the interstitial electron density in crystalline metals and some ground-state properties, including the compressibility, we propose a procedure to estimate the interstitial electron density in liquid metals starting from the experimental static structure factor. From the calculated electron density, starting from the standard approximation, which describes a liquid metal as made up of a homogeneous classic ion plasma with Coulomb interaction and a homogeneous interacting electron gas, we determine the ion collective mode velocity. The so-derived collective mode velocity is compared to the experimental data and a coherent view in different metallic systems at the melting point is obtained. Some guess about the collective mode damping is also presented because of the connection to the local static fluctuations of the interstitial electron density.

DOI: [10.1103/PhysRevB.90.024207](https://doi.org/10.1103/PhysRevB.90.024207)

PACS number(s): 61.25.Mv, 71.22.+i, 05.30.Fk, 52.27.Gr

## I. INTRODUCTION

The study of the high-frequency ion dynamics of liquid metals has been the subject of several theoretical and experimental investigations because of its basic interest and the possibility of deriving valuable information on the electron-electron and ion-electron interactions [1–14]. Despite the copious information that is now available, it is not yet clear how to correlate the experimental results and the theoretical approaches, even if the electron-electron interaction can be investigated as the ions act like a (weak) probe in the electron fluid. Indeed, the propagation of well defined collective ion modes in liquid metals can be described using a two component model of the system, a model simple enough for analytic approximations. The relevance of the interacting electron fluid in liquid metals is well enhanced by the surprising case of lithium ammonia solutions, a very low electron density system that shows quite an anomalous collective mode dispersion curve [11,12] and damping [13]. Although the two-component model of the liquid metal is an appealing one, a rather basic aspect has been left out. The electron fluid is modeled using a homogeneous electron gas the density of which cannot be easily determined from the known property of the system apart from the case of alkali metals, where it is safely assumed that the electron gas is generated by uniformly distributing one electron per atom. In general, the possibility of a well defined comparison of different systems is limited as there is no straightforward way to determine the electron gas density and the proper ion charge. In this paper, we propose an approach that can be used for a uniform description of different liquid metals by using some experimental information on the structure of the liquid to infer the proper electron gas density.

Long time ago, it was recognized that the compressibility of crystalline metallic elements follows an empiric trend as a function of the interstitial electron density [15] similar to that of the compressibility of the noninteracting homogeneous electron gas [16]. This empiric observation is almost equivalent at stating that the compressibility of solid metals is dominated

by the compressibility of the interstitial electrons treated as noninteracting.

However, one has to notice that real systems are stable even at rather low interstitial electron density like that of Cs, where the interstitial electron density is smaller than the critical density  $n_c$  where the compressibility of the interacting electron gas becomes negative. This observation, as expected, shows that the shape of the ion potential plays an important role in determining the compressibility of solid metals. More recently, it has been shown that the density of interstitial electrons is relevant in determining various properties of a metal [17,18] in the crystalline phase. These observations are of interest in crystalline systems in order to understand also on a semiquantitative ground the origin of the trends observed in the solid state, once the electron gas and the ionic potential are treated with the appropriate approximation. On the other hand, thanks to the lattice periodicity, in a crystalline system, one can efficiently apply the density functional theory (DFT) based approximations, used for first-principles derivations of various properties, including fine details like lattice dynamics [19]. Therefore the interstitial electron density is no more of major practical importance in crystalline solids. On the contrary, in disordered systems, the direct application of the DFT approach is difficult and limited by the size of the system that can be efficiently treated. In addition, the identification of general trends is not straightforward and even the behavior of simple quantities is not well understood.

At present, ground to a two-component approach is given by the experimental evidence that an almost uniform electron gas affects the ion-ion interaction in various liquid metals [8–10], which are prototypes of simple disordered systems. Accordingly, these liquid metals can be approximated by a *strongly* interacting ion plasma embedded into an interacting electron gas that acts as a *linear* screening medium for the bare ion-ion interaction [20]. As is well known, this point of view is an old one and it has been the basis of several studies of the phonon dispersion relations in crystals [5,19,21], while in disordered systems, it has been used in the seminal work of

Bardeen and Pines [3] and several other investigations [6,7,22], including the standard textbooks by Pines and March [1,2].

With reference to the two-component approximation for the liquid metal, the two components interact with each other through an appropriate ion-electron potential. When this two-component system is treated in the weak ion-electron interaction limit, it is found that it sustains collective ion density fluctuation modes that propagate with a velocity given by the well-known Bohm-Staver formula [2],  $c_{BS} = (m/M)^{1/2}v_F$ ,  $m$  and  $M$  being the electron and ion masses, respectively, and  $v_F$  the Fermi velocity. This approach has some validity in the long-wavelength limit but at high enough frequency as compared to the characteristic relaxation time of the system.

In this paper, we develop a method appropriate to calculate the proper electron density and ion charge to be used to apply the Bohm-Staver formula, properly extended according to the discussion reported in Refs. [2,9,12], to calculate the collective mode velocity of different liquid metals. We introduce a procedure that can be applied in systems having any electron configuration compatible to the use of the two-component approximation. In general, such an approximation can be expected to be correct in many metals apart from those where  $d$ -like states are occupied.

In the following, we present a calculation that is performed starting from the known mass density of the system, the total number of electrons per atom, and the experimentally determined microscopic structure, that is, the static structure factor. No other input information is required and the procedure is successfully applied to the case of liquid alkali metals and polyvalent metals. We discuss the ion contribution to the velocity of the collective modes, using an appropriate approximation scheme for the strongly interacting ion plasma [23] and an accurate approach for the response of the electron fluid [24]. By comparing the present description with the experimental findings, we can extract some general view on the collective mode propagation in liquid metals and some validation of both electron gas and ion plasma theoretical knowledge.

## II. CALCULATION OF THE ELECTRON GAS DENSITY

In this section, we present the protocol we propose to determine the electron gas density from the experimental structure of the liquid metals as described by the static structure factor  $S(Q)$ , which is the Fourier transform of the ion-ion pair correlation function. We recall that the two-component model is based on the uniform electron gas with no ions and positive rigid background plus the ion plasma with a rigid negative background used to make the system neutral. Then the *screened* ion-electron interaction is introduced to describe the ion density fluctuations [2,3]. In this way, the electron density fluctuations due to the ions are introduced by the ion potential screened by the electron gas.

To determine the proper electron gas density, we assume that the effective electron density is equal to the average electron density found in the interstitial region. The ion charge is then derived from the system neutrality. Therefore it is necessary to determine the *configurationally averaged* electron density in the liquid system. In principle, in a liquid

elemental system, the electron density can be determined by means of x-ray diffraction, however, in practical cases, this approach is never used because an accurate experiment implies a measurement extending up to very high momentum transfer beyond any reasonable value. Moreover, this sort of experiment is normally used to derive some information on the local atomic arrangement. When x-ray diffraction is used, the scattering factor deduced from atomic calculations [25] is employed to derive an accurate static ion-ion structure factor  $S(Q)$  from the diffracted intensity. Notice that this approach is known to be correct as the static structure factor  $S(Q)$  determined by means of x-ray diffraction is in general agreement with that obtained by neutron scattering where the ion-ion structure factor is directly determined. Therefore it is reasonable to state that the actual electron density distribution is well described from the static structure factor and the atomic scattering factor.

The use of the calculated atomic scattering factor is rather appropriate since the difference between the actual scattering factor and that of the corresponding free atom is small as it is well supported by the experiments performed in some crystals where the scattering factor can be accurately measured. It is seen that the crystal scattering factor differs from that of the free atom by a small amount confined in the small momentum region [25] only, so that the difference between the actual electron density and that derived from the simple superposition of free-atom electron density is spread out through the unit cell.

Accordingly, we study the electron density in a liquid metal assuming that it can be approximated by a superposition of free-atom electron densities using the atomic distribution experimentally determined from the pair distribution function  $g(r)$ , which is proportional to the Fourier transform of the static structure factor  $S(Q)$ . Notice that this approach is formally exact in the case of x-ray scattering and contains a small approximation in the case of neutron scattering. Therefore the *configurationally averaged* electron density  $\langle\rho(r)\rangle$  centered about a central atom is determined by making use of the pair correlation functions determined from the experimental static structure factor. We have

$$\langle\rho(r)\rangle = \rho_{at}(r) + n^{(i)} \int g(|\mathbf{r} - \mathbf{r}'|) \rho_{at}(r') d\mathbf{r}', \quad (1)$$

where  $n^{(i)}$  is the ion density and  $\rho_{at}(r)$  is the (spherical) free-atom electron density. Considering that  $4\pi r^2 g(r)$  is the probability density of finding an atom at distance  $r$  from an atom located at the origin, after some algebra one obtains the following equation that might be suitable for the actual calculation:

$$\langle\rho(r)\rangle = \rho_{at}(r) + Zn^{(i)} + \frac{1}{2\pi^2 r} \int [S(Q) - 1] \times f(Q) Q \sin(Qr) dQ, \quad (2)$$

where  $Z$  is the atomic number. Equation (2) provides the average electron density at  $r$ , however, for a correct determination of the proper electron gas density, we assume to use  $\langle\rho(r)\rangle$  averaged over the interstitial region. To this purpose, starting from Eq. (2), we determine the number of electrons  $Z_R$  inside

a sphere of radius  $R$  centered about the central atom. We have

$$Z_R = \Omega(R) Z n^{(i)} + \frac{2R}{\pi} \int_0^\infty dQ f(Q) [S(Q) - 1] J(QR) + \frac{2R}{\pi} \int_0^\infty dQ f(Q) J(QR), \quad (3)$$

where  $\Omega(R)$  is the volume of the sphere of radius  $R$  and the function  $J(x)$  is given by  $J(x) = [\sin(x) - x \cos(x)]/x$ . Starting from Eq. (3), the average interstitial electron density is determined from the following relationship:

$$\langle \rho_{\text{gas}} \rangle = \frac{Z - Z_{\bar{R}}}{\Omega_i - \Omega(\bar{R})}, \quad (4)$$

where  $\Omega_i = 1/n^{(i)}$  is the average ion volume and  $\bar{R}$  is the average ion touching radius, which can be approximated by the distance where  $\langle \rho(r) \rangle$  is minimum.

In practical situations, Eqs. (2), (3), and (5) are not very useful since the integral implies the knowledge of  $S(Q)$  in an extremely wide range of  $Q$ ,  $f(Q)$  being appreciably different from zero up to very high momentum values, well beyond the possibility of any realistic experiment. In addition,  $S(Q) - 1$  is an oscillating function of  $Q$  and it is not possible to assume that it is equal to zero when  $Q$  exceeds some maximum value because such a procedure introduces relevant termination errors. In order to avoid this problem, we make use of the fact that in all atoms the electron density can be reasonably split as the sum of two contributions: a core electron contribution, which is sharply peaked around the atomic nucleus, and a valence electron contribution, which is much more spread out. This separation has not a solid formal ground but it is empirically correct. It should be mentioned that the distinction between core and valence states is used also to develop the pseudopotential approximation [19,26], which is quite efficient in many solid state calculations. Starting from this observation, we can write the atomic scattering factor as the sum of the two contributions belonging to the core states and the valence states, respectively:

$$f(Q) = f_c(Q) + f_{\text{val}}(Q).$$

Inserting this relation into Eq. (2), we can derive the following form for the central atom electron density in the interstitial region where we assume the presence of a negligible contribution coming from the core electrons of the central atom and of all nearby atoms:

$$\langle \rho(r) \rangle = \rho_{\text{at}}(r) + Z n^{(i)} + \frac{1}{2\pi^2 r} \int [S(Q) - 1] \times f_{\text{val}}(Q) Q \sin(Qr) dQ. \quad (5)$$

The last term does not contain the total scattering factor since one can make use of the fact that no core electron can contribute to the electron density at such large distance  $r$  from the central atom, since this position has a distance that is similar or larger than  $r$  from all the other atoms. This result follows from the following formal relationship based on such an approximation:

$$\int_0^\infty [S(Q) - 1] f_c(Q) \sin(Qr) Q dQ = -2\pi^2 r Z_c n^{(i)}, \quad (6)$$

where  $Z_c$  is the number of core electrons and  $r$  is in the interstitial region between the central atom and those being

nearest neighbors. Using Eqs. (5) and (6), one can write the following equation, which is more useful for practical applications since  $f_{\text{val}}(Q)$  decays much faster than  $f(Q)$  on increasing  $Q$ :

$$Z - Z_R = Z_{\text{val}} - \left\{ n^{(i)} Z_{\text{val}} \Omega(R) + \frac{2R}{\pi} \int_0^\infty dQ \times f_{\text{val}}(Q) [S(Q) - 1] J(QR) + \frac{2R}{\pi} \int_0^\infty dQ f_{\text{val}}(Q) J(QR) \right\}. \quad (7)$$

In order to evaluate the electron gas density using the above equations, we have to determine first an appropriate valence scattering factor. In principle, one could derive the valence contribution from the one-electron wave functions. However, we prefer an alternative and simpler procedure based on the fact that it is possible to derive a good estimate of  $f_{\text{val}}(Q)$  by subtracting from  $f(Q)$  an approximate core electron scattering factor. This choice is related to the fact that the best calculation of the atomic scattering factor is that of Hubbell and Øverboø [25,27], and it is not obvious how to deduce the corresponding core contribution. We observe that the exact shape of the core electron contribution is not relevant to the purpose of determining the interstitial electron density, provided that the corresponding charge is  $Z_c$ . In other words, any sharply peaked electron density function with total charge equal to  $Z_c$  verifies Eq. (6) so that Eq. (5) is also valid. Of course, it is important also to use an approximation  $f_c^a(Q)$  such that  $|f_c^a(Q) - f_c(Q)|$  is negligible in the high- $Q$  region where the static structure factor is unknown. We found that an approximate core electron scattering factor, having the correct behavior, can be obtained from a properly rescaled electron density of the first noble gas located in the periodic table before the atom we are considering. Therefore, in order to perform the calculation, we used a valence electron scattering factor  $f_{\text{val}}(Q) = f(Q) - f_N(KQ)$ ,  $f_N(KQ)$  being the rescaled scattering factor of noble gas. The scaling constant  $K$  can be derived by minimizing the average value of  $|f(Q) - f_N(KQ)|$  at high  $Q$ . We find that it is better to use the present approximation instead of using the scattering factor of some ionic state of the atom because the shape of the electron distribution in the ion is deformed as compared to that of the neutral atom. This is due to the absence of the valence electron screening effects in the free ion. In addition, ions with fractional charge are difficult to be considered.

To demonstrate the basic idea behind the above procedure, in Fig. 1, we show the scattering factors of two metals, namely, Zn and Bi, as compared to the scaled scattering factors of the noble gases Ar and Xe, which compare very well to those of the metals in the high- $Q$  region where the  $f_c(Q) = f_N(KQ)$  is very close to  $f(Q)$ . Of course, the electron densities of Ar and Xe do not extend over a wide range because they are closed shell atoms and due to the scaling factors  $K = 0.580$  for Ar and  $K = 0.550$  for Xe, the effective core density for Zn and Bi is even more contracted thus spanning a small range in space. Of course, the core electron density is more contracted in Zn and Bi than in Ar and Xe as the atomic number is higher in the metal so that the inner electrons states are more tight bound to the nucleus.

As specified before, the scattering factors are those tabulated in a very extended  $Q$  range by Hubbell and Øverboø

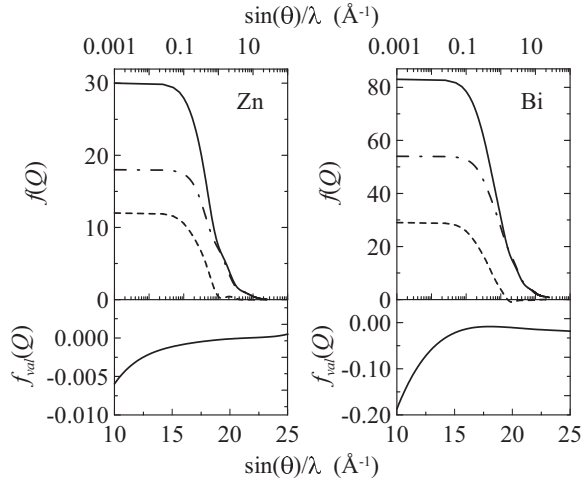


FIG. 1. (Top) Atomic scattering factor of Zn and Bi as compared to the scaled scattering factor of Ar and Xe, respectively, as a function of the momentum transfer as measured by  $\sin(\theta)/\lambda = Q/4\pi$ . The logarithmic scale is used for  $Q$  to show the region where the scattering factors become small. (Bottom)  $f_{\text{val}}(Q)$  is plotted in the high- $Q$  region in order to show the good convergence of  $f_N(KQ)$  to  $f(Q)$  as  $f_{\text{val}}(Q)$  is rapidly approaching zero.

[27] based on relativistic Hartree-Fock one-electron wave functions, which have been proved to be quite accurate in the high-momentum region in crystals [25]. The scaling factor  $K$  is determined in a very high  $Q$  range from 100 to 200  $\text{\AA}^{-1}$ , while  $|f(Q) - f_N(KQ)|$  is close to zero typically when  $Q$  is higher than 10–20  $\text{\AA}^{-1}$ , a range that is accessible to experiments devoted to the measurement of the static structure factor  $S(Q)$ .

In the numerical calculation, to determine the ion charge  $Z_i$  we observe that the average electron density at  $R$  located in the interstitial region  $\langle\rho(R)\rangle$  can be obtained by means of the following equation:

$$\langle\rho(R)\rangle = -\frac{1}{4\pi R^2} \frac{d(Z - Z_R)}{dR}. \quad (8)$$

To numerically determine the derivative in Eq. (8),  $Z_R$  was fitted using an eighth degree polynomial, which allows for a simple analytic derivation and reduces the effect of small numerical errors, which are of the order of 0.01 % in all cases. This procedure is numerically more efficient than the direct calculation. Once  $\langle\rho(R)\rangle$  is calculated, we determine the position  $\bar{R}$  of the density minimum, which can be used to evaluate the interstitial electron density according to Eq. (4). Once the electron gas density is obtained from the charge neutrality:

$$Z_i = \langle\rho_{\text{gas}}\rangle\Omega_i. \quad (9)$$

Considering that the procedure used to derive Eqs. (5) and (8) contains some approximation to make the calculation feasible, we first tested the validity of the approach by checking the calculation in the case of a *hypothetic* liquid Bi having the static structure factor  $S(Q)$  as determined by the analytic Percus-Yevick approximation at the same density of the real liquid metal and at the appropriate packing fraction to produce a  $S(Q)$  as similar as possible to the experimental one. We used an atomic size  $\sigma = 3.05 \text{\AA}$  and the resulting  $S(Q)$  is

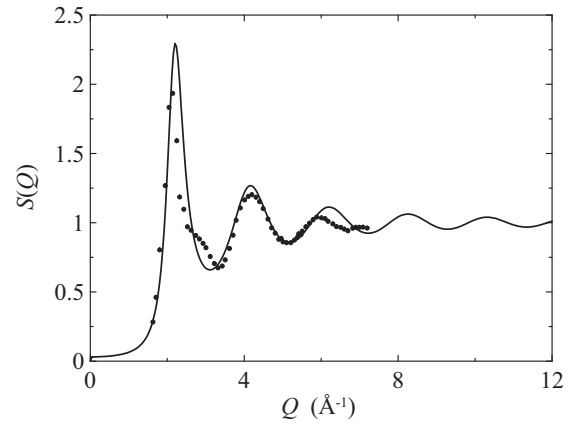


FIG. 2. Percus-Yevick approximation of the Bi structure factor (full line) as compared to the experimental results [28] (dots).

reported in Fig. 2 in comparison with the experiment [28]. A packing density parameter is  $\eta = 0.43$ , a value which is typical for metals, like alkali metals. Of course, the Percus-Yevick approximation cannot catch the details of liquid Bi as the real metal shows a complex behavior in the region of the first peak where there is a secondary bump. This bump can be related to the  $2k_F$  singularity of the electron gas dielectric function [2], which can account for the well known Friedel oscillations in the atom-atom effective potential. This hypothetic system was chosen to compare the calculation performed using both the approximate method of Eq. (5) and the formally more accurate approach of Eq. (2). Of course, such a hypothetic system is not equal to the actual liquid Bi, but it can be employed as a test to determine the size of the errors introduced by the limited knowledge of  $S(Q)$  in the case of real systems where  $S(Q)$  is determined using some experimental approach. Considering that Bi has a very large number of electrons per atom, in this test, one is maximizing the expected error introduced by the approximate scheme of Eq. (5). We calculated the spherically averaged electron density as deduced from Eq. (2) and from the approximate Eq. (5) in the hypothetic liquid Bi. The so determined electron densities are reported in Fig. 3, where we see, as expected, a region with an almost constant electron density and the same result from Eqs. (2) and (5). In the inset of Fig. 3, we report also  $Z_R$  as a function of  $R$ , according to Eqs. (2) and (5). Using the approximate approach of Eq. (5), all the contributions to the integral above  $Q_M = 20 \text{\AA}^{-1}$  have been neglected as it is the case for a real system where  $S(Q)$  is known in a limited momentum range. From these results, an electron gas density  $\rho_{\text{gas}} = 0.077 \text{ electrons/\AA}^3$  and hence an ionic charge  $Z_i = 2.67$  are obtained.

According to this calculation, which is performed in the case of a high atomic number atom, we can safely argue that the scheme proposed in Eq. (5) is adequate for defining a proper protocol to obtain a good estimate of the effective ion charge or the interstitial electron density.

A different protocol within the same two-component model for the liquid metal was employed in Ref. [14] to determine the interstitial electron density. This protocol was based on the assumption that the interstitial electron density of the liquid is equal to that calculated in a compact crystal, e.g., either fcc

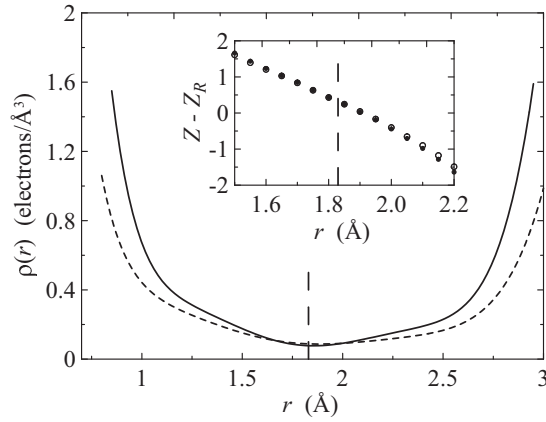


FIG. 3. Electron density  $\langle\rho(r)\rangle$  as a function of the distance from the central atom in the hypothetic liquid Bi in the Percus-Yevick approximation (see text). The full line refers to the calculation performed using the full scattering factor as in Eq. (2). The dashed line is the result obtained using Eq. (5), which includes the valence electrons only. In the inset, the integrated charge difference  $Z - Z_R$  is shown using the charge density as determined using the two approximations. In the all-electron calculation,  $Z$  is equal to the nuclear charge (full dots), in the valence-electron calculation  $Z = Z_{\text{val}}$  (circles).

or bcc, having the same density as the liquid. To perform this calculation again, it is assumed that the electron density of the crystal used to mimic the liquid is given by the superposition of free-atom electron densities located at the lattice sites and the interstitial electron density is derived by taking the average density within the interstitial volume defined as the volume of the unit cell left out by touching atomic spheres. This approximation neglects completely the actual structure of the liquid but it has the advantage of computational simplicity. In this approximation, the interstitial electron density is derived from the number of the interstitial electrons determined by the difference between the atomic number and the number of electrons inside an atomic sphere. The final result is quite simple as, given the number of interstitial electrons  $Z_{\text{int}}$ , the interstitial electron density is given by

$$\langle\rho_{\text{gas}}\rangle = \frac{Z_{\text{int}}}{\Omega_{\text{int}}} = \frac{Z - n^{(i)} \sum_{\mathbf{G}} f(\mathbf{G}) J(\mathbf{G} R_a) R_a / G^2}{\Omega_{\text{int}}}, \quad (10)$$

where the sum runs of the reciprocal lattice vectors,  $R_a$  is the radius of the atomic sphere, and  $\Omega_{\text{int}} = \Omega_i - 4\pi/3 R_a^3$  is the interstitial volume. The radius of the atomic sphere is easily derived from the density of the crystal, which is assumed to be that of the liquid. Within this approximation, the system structure is exactly known because it is defined by the crystalline phase one is using. Interestingly, in the case of simple systems like alkali metals or alkali earth metals, this approximation provides an ion charge very close to one and two, respectively [14]. However, in more complex systems where the actual structure is not very compact, this simple approximation is expected to be less adequate than the approach that takes into account the actual structure of the liquid.

### III. PROPAGATION OF ION DENSITY FLUCTUATIONS

The description of a liquid metal as a two-component system, where the ions are embedded into a uniform electron gas, is an approach which has been first applied long time ago. In this approximation, one assumes that the ions have an average number density  $n^{(i)}$  and a charge  $Z_i e$  and, since the system is neutral, the electron number density is simply obtained as  $n = Z_i n^{(i)}$ . Here, we just report the basic results concerning the collective dynamics of the two-component system as it has been developed before [1–3,6,7,29]. Once a liquid metal is described as a uniform interacting electron gas where ions are uniformly distributed, one can study the ion density fluctuations within the linear response theory [2,29], that is, by determining the *screened* ion-electron potential. In a phononlike approach, the *longitudinal* density fluctuations having a wave vector  $\mathbf{q}$  have eigenfrequencies given by

$$\omega_c^2(q) = \Omega(q)^2 - \Omega_p^2 F(q) \left[ 1 - \frac{1}{\epsilon(q)} \right], \quad (11)$$

where  $\Omega(q)$  is the frequency of the longitudinal density fluctuations of the interacting ion plasma and  $\Omega_p^2 = 4\pi(Z_i e)^2 n^{(i)} / M$  is the ion plasma frequency,  $F(q)$  is the form factor of the bare ion-electron interaction potential, and  $\epsilon(q)$  is the (static, i.e., low frequency) dielectric function of the uniform electron gas at the appropriate density. This equation, which is valid only at high enough frequency, was reported long time ago in the standard textbook of Pines [1] and it has been used in other investigations [10,12,13]. The effect of the finite ion size and the momentum dependence of the eigenfrequencies of the bare ion plasma  $\Omega(q)$  are explicitly indicated even if this is a low-momentum approximation. When pointlike ions are considered, the usual Bohm-Staver relationship is obtained because  $F(q) \simeq 1$ ,  $\Omega(q)^2 \simeq \Omega_p^2$  and  $\epsilon(q) \simeq 1 + k_s^2 / q^2$ ,  $k_s$  being the screening wave vector of the electron gas. To deduce the original Bohm-Staver approximation, one has to use the random phase approximation (RPA) approximation, namely,  $k_s^2 \simeq k_{\text{TF}}^2 = 6\pi n e^2 / k_F^2$ , as the Thomas-Fermi wave vector  $k_{\text{TF}}$  is the screening wave vector in this limit.

Notice that still in the pointlike ions limit and with the approximation  $\Omega(q)^2 \simeq \Omega_p^2$ , the velocity of collective modes is modified with respect to the Bohm-Staver equation by the presence of the electron-electron interaction [10,14], which changes the screening wave vector, thus obtaining an electron only exact result  $c_{\text{ex}}$  beyond the RPA, that is,

$$c_{\text{ex}} = \lim_{q \rightarrow 0} \frac{\omega_c}{q} = \frac{\Omega_p}{k_s}, \quad (12)$$

where the electron gas screening wave vector  $k_s$  can be exactly derived from the compressibility sum rule. One has

$$k_s^2 = \frac{k_{\text{TF}}^2}{1 - \lambda k_{\text{TF}}^2}, \quad (13)$$

where the  $q^2$  coefficient  $\lambda$  of the small  $q$  expansion of the zero-frequency local field is given by the following *exact* equation [24]:

$$\lambda = \frac{1}{4k_F^2} \left( 1 + \frac{\pi}{3} \alpha_g r_s^2 \frac{\partial \epsilon_c}{\partial r_s} - \frac{\pi}{6} \alpha_g r_s^3 \frac{\partial^2 \epsilon_c}{\partial r_s^2} \right), \quad (14)$$

where  $\alpha_g = (4/9\pi)^{1/3}$  and  $a_0 r_s = (3/4\pi n)^{1/3}$  is the electron gas density parameter,  $a_0$  being the Bohr radius. Here, it is necessary to know the energy per particle of the electron gas or the correlation energy per particle  $\epsilon_c$ , which is available from quantum Monte Carlo calculations [30,31].

It is quite important to observe that  $k_s^2$  is not a positive defined quantity as a function of electron gas density as at the critical density  $n_c$  the electron gas compressibility becomes negative. Such a critical electron density is higher than that of liquid Cs and rather close to that of Rb, therefore at least in these systems the ion-electron interaction must give quite a relevant contribution, which determines the stability and the velocity of the density fluctuations. Therefore one has also to consider the effect of the form factor of the ion-electron potential even in the small-momentum limit.

As is well known, the collective mode velocity can be probed experimentally by means of inelastic scattering of neutron or x ray, so that a proper comparison between theory and experiment can be readily performed. In the  $q \rightarrow 0$  limit, the following approximations can be safely applied:

$$\begin{aligned}\Omega(q) &= \Omega_p[1 + \delta_p(q/q_d)^2 + \mathcal{O}(q^4)], \\ F(q) &= 1 - (\langle R^2 \rangle / 6)q^2 + \mathcal{O}(q^4),\end{aligned}\quad (15)$$

where  $q_d^2 = 4\pi n^{(i)}(Z_i e)^2 / k_B T$  is the Debye wave vector,  $\delta_p$  is a parameter describing the ion plasma dispersion relation at small wave vector [23], and  $\langle R^2 \rangle$  is the mean square radius of the ion-electron interaction potential. The collective mode velocity  $c$  is readily obtained using these approximations [14]:

$$c^2 = \lim_{q \rightarrow 0} \frac{\omega_c^2(q)}{q^2} = c_{\text{ex}}^2 + \Omega_p^2 \left( \frac{2\delta_p}{q_d^2} + \frac{\langle R^2 \rangle}{6} \right). \quad (16)$$

We see that the calculation of  $c$  requires only the knowledge of the ion charge  $Z_i e$ , of  $\delta_p$  and  $\langle R^2 \rangle$ . For the sake of simplicity, we will use

$$\alpha = \frac{2\delta_p}{q_d^2}, \quad \beta = \frac{\langle R^2 \rangle}{6}. \quad (17)$$

Equation (16) is already reported in Refs. [2,4], here we have just presented the relevant contributions, which will be used in the systematic comparison with a set of experimental data. We note also that the electron gas screening, which determines the effective ion-ion potential, is described by the screening wave vector  $k_s$  used to calculate  $c_{\text{ex}}$ . In the present  $q \rightarrow 0$  limit, no details of the ion-ion interaction such as the Friedel oscillations, which have a frequency equal to  $2k_F$ , have a strong weight. Some subtle effect, possibly related to the  $2k_F$  singularity, or to the exact shape of the ion-electron interaction, has been observed at finite momentum [11–13].

All the above equations contain two relevant parameters, namely, the electron density parameter  $r_s$  of the interstitial electrons and the ion density parameter  $a_0 R_i = (3/4\pi n^{(i)})^{1/3}$ , which are the basic input quantities defining the two systems, namely, the electron gas and the ion plasma. The two parameters  $R_i$  and  $r_s$  are related to each other through the ion charge in the following way:

$$R_i = Z_i^{1/3} r_s,$$

so that the relevant quantity to be determined is either  $r_s$  or  $Z_i$ , while  $R_i$  is obtained from the experimental density.

#### IV. CALCULATION OF THE ELECTRON GAS DENSITY PARAMETER IN REAL METALS

According to the procedure, we outlined in Sec. II, we made the calculation of the interstitial electron density in a series of sixteen liquid metals chosen as representative of the different elements of the periodic table and such that experimental values of the collective mode velocity are also available [8–10,32,33]. We employed the procedure based on Eq. (8) and all the calculations have been performed using the atomic scattering factors of Ref. [27], while the experimental static structure factors  $S(Q)$  [28,34] have been used. We first calculated the ion charge  $Z_i$  and the electron gas density parameter  $r_s$  according to Eq. (4).

The results of the described procedure are reported in Table I where we report also other relevant parameters. We see that the electron density parameter derived from the liquid is generally in fair agreement with that obtained in the crystalline solid in Ref. [35] or by determining the number of  $s + p$  electrons from the band structure calculations [36]. In the case of simple systems, the results are also in agreement with those derived by means of the crystalline approximation used in Ref. [14].

In the case of a simple metal like Al, we calculate  $Z_i = 2.82$  against 3 ( $s + p$ )-like electrons according to the free-atom configuration, in the shell model. The same result is obtained with the crystal calculation [14] and band calculation [36]. The explanation for the small difference between  $Z_i$  and the atom valence could be related to either the use of the free-atom scattering factor or to a real difference between the free-atom and the liquid metal. Of course, we cannot avoid the use of the free-atom scattering factor in the calculation and the comparison with the number of electrons in the free atom should be taken with some care since the electron states in the liquid metals are probably more spread out. We remark

TABLE I. Ion density parameter  $R_i$ , ion charge  $Z_i$ , and electron density parameter  $r_s$  derived in the liquid from the present calculation. For comparison purposes the results reported in Refs. [14,35,36] are also shown. The results obtained from Ref. [36] are calculated using both the solid and liquid densities.

Element	$R_i$	$Z_i$	$r_s$	$r_s$ [14]	$r_s$ [35]	$r_s$ [36]	solid $r_s$ [36]	liquid
Li	3.30	1.05	3.249	3.250	3.61	3.270	3.325	
Na	4.01	1.01	4.000	4.014	4.01	4.006	4.028	
K	5.01	1.07	4.903	4.889	4.67	4.924	5.062	
Rb	5.39	0.95	5.478	5.204	4.68	5.309	5.481	
Cs	5.78	0.94	5.904	5.586	5.10	5.783	5.953	
Ca	4.27	1.95	3.416	3.230	3.42	3.661	3.789	
Ba	4.79	1.72	3.997	3.532	3.69	4.539	4.650	
Al	3.11	2.82	2.204	2.191	2.51	2.076	2.175	
Si	3.10	3.38	2.064	–	–	–	–	
Ge	3.28	3.19	2.230	2.550	–	–	–	
Ga	3.16	2.78	2.248	2.426	2.63	2.161	2.232	
Sn	3.57	3.08	2.454	2.637	–	–	–	
Cd	3.35	2.02	2.650	2.552	2.74	2.578	2.694	
Hg	3.40	2.66	2.451	2.835	3.02	–	–	
Pb	3.74	3.13	2.557	2.962	2.78	2.305	2.358	
Bi	3.82	3.30	2.565	3.124	–	–	–	

again that when the static structure factor derived from an x-ray diffraction measurement is used, the present approach is expected to be much more accurate. Indeed,  $S(Q)$  is derived by normalizing the scattered intensity to the free-atom scattering factor in the case of the x-ray diffraction. Therefore apart from other approximations intrinsic to the experiment and the calculation, no error is introduced by the use of the free-atom data. It is important to note also that the scattering factor used in the most part of the x-ray experimental investigations is that of Ref. [27] so that there is no additional approximation connected to the use of different theoretical results.

To check the order of magnitude of the error introduced by using the free-atom scattering factor when  $S(Q)$  from neutron scattering is used, we consider again the case of Al, which can be expected to be a difficult one because it has about three valence electrons having a scattering factor that extends in a rather wide  $Q$  range. We made a simple test by performing the calculation using a corrected scattering factor  $f_{\text{cor}}(Q) = f(Q) + \Delta(Q)$ , where  $\Delta(Q)$  was deduced from the comparison of the experimental data in the crystal [37] to  $f(Q)$ . Of course, we assume that the difference  $\Delta(Q)$  is similar in the liquid and solid states, an approximation which we consider acceptable. Using this procedure, which suggests  $\Delta(Q) \simeq -0.07Q^2 \exp(-0.19Q^2)$  with  $Q$  in angstrom units, we got  $Z_i = 2.62$  against  $Z_i = 2.82$  previously obtained. This result has a minor dependence on the exact form used to evaluate  $\Delta(Q)$  and on the detailed form of  $S(Q)$ . We mention also that the expected difference between the free atom electron density and that of a condensed system like a liquid metal cannot be very large because this difference is related to the cohesive energy [25]. As a consequence, we can safely state that the value of  $Z_i$  has a maximum error of the order of one or two tenth of electron. It is interesting to observe that this corrected result is even more different from the simple estimate  $Z_i = 3$  than that derived using the free-atom scattering factor.

Looking at Table I it is also interesting to consider the trend of the ion charge along the periodic table. Indeed, as expected, the alkali metals show a charge very close to unity, according to the idea that only one electron is available for the electron gas. The alkali-earth metals, Ca and Ba, also show a charge of about 2, while Si, Ge, and Sn seem to have a lower ion charge than the nominal valence, i.e.,  $Z_i = 4$ , with the tendency of decreasing  $Z_i$  from 3.38 in the case of Si to 3.08 in the case of Sn. It should be mentioned that  $Z_i = 4$  is a value related to the diamond structure where there is an  $s$ - $p$  hybridization, while the liquids show a quite different behavior due to their metallic character. Finally, a rather complex trend is seen in the case of polyvalent metals Cd, Sn, Hg, Pb, and Bi, where the ion charge is higher than the number of nominal valence electrons in Hg, while it is smaller in Sn, Pb, and Bi.

Considering the results of Table I, we believe that the proposed procedure provides an adequate determination of the interstitial electron density in a liquid metal, useful to make a meaningful comparison of different systems.

## V. CALCULATION OF THE COLLECTIVE MODE VELOCITY

According to the previous sections, we use the so determined ion charges to estimate the collective mode velocity

and to compare the results to the experimental findings. In order to have a uniform and meaningful comparison, all the experimental data of inelastic neutron and x-ray scattering have been analyzed in terms of a standard empiric model, which includes a quasielastic peak and an inelastic contribution approximated by a damped harmonic oscillator response. The most part of the experimental results is the same as in Ref. [14], however, the results for Al have been corrected because of a misprint and for Cd because of a better analysis of the experimental data in the case of this system [8,32].

According to the discussion of the previous section and Ref. [10], the screening wave vector  $k_s$  can be derived from an accurate determination of the electron gas correlation energy [30,31]. On the other hand, if one neglects the two parameters  $\alpha$  and  $\beta$ , that is, the last two terms in the right-hand side of Eq. (16), one obtains a collective mode velocity which is determined by the electron gas properties only. This estimate is expected to be meaningful when there is a high electron density, however, as already discussed, the velocity as deduced from the electron gas only becomes imaginary when the density is low, i.e., when  $r_s > 5.45$ . Therefore the low-density systems are stable, i.e., a real velocity of the collective modes is deduced, because of the sizable contribution from the ion interactions. We mention that already at  $r_s = 2$ , the size of the local field effect on the collective mode velocity is of the order of 20 % as it is seen in Table II. Therefore the simple Bohm-Staver approximation cannot be applied to real systems and as we will see all the terms are important because the various contributions compete each other.

Considering that the collective mode velocity depends only on the sum  $\alpha + \beta$ , our strategy was to first derive some information by comparing Eq. (16) to the available experimental data. We calculate an *experimental*  $\alpha + \beta$ , by assuming that the electron gas contribution can be calculated according to the above prescriptions. This is the same strategy used in previous investigations [10,14] where a simple approach was used to determine the electron gas density. The results obtained using this procedure are reported in Table II where the elements are grouped in such a way that some simple trend is visible within a given class of systems. In addition, these results are presented in Fig. 4, where it is seen that the experimental estimate of  $\alpha + \beta$  shows a trend as a function of  $R_i$ . This trend suggests that the ion dependent quantities  $\alpha$  and  $\beta$  are mainly related to the ion density.

To obtain a theoretical determination of the collective mode velocity without additional experimental information, one has to calculate the two parameters  $\alpha$  and  $\beta$  that represent the contribution of the ion plasma dispersion and the ion finite size. There is no simple general way to determine these two parameters. The calculation of  $\delta_p$  is rather complex, as it is known only in the homogeneous plasma in the weak interaction limit, that is, when the coupling constant [23]  $\Gamma = (Z_i e)^2 / ak_B T \ll 1$ . In this limit, the RPA [23] applies, so that  $\delta_p = 3/2$ . However, the ion plasma in liquid metals is always in the strong coupling limit, that is,  $\Gamma \gg 1$ . An exact calculation of  $\delta_p$  in the strong coupling limit is not yet available, but various approximations have been proposed for  $\delta_p$  in the past either from analytic approximations or from molecular dynamics simulations [23]. A simple useful

TABLE II. Collective mode velocity obtained using different approximations and ion parameters  $\alpha$  and  $\beta$  (see text). The velocity  $c_{\text{RPA}}$  is the RPA estimate of the collective mode velocity, that is, when  $k_s = k_{\text{TF}}$ ,  $c_{\text{ex}}$  is the estimate deduced considering the correct expression for  $k_s$  (see text), and  $c_{\text{exp}}$  is the experimental value. Notice the imaginary value of  $c_{\text{ex}}$  in Rb and Cs, which have an electron density smaller than the critical value. The value of  $(\alpha + \beta)_{\text{exp}}$  is evaluated *experimentally*, comparing the theoretical value for  $c_{\text{ex}}$  to the corresponding experimental value (see text).

Element	$c_{\text{RPA}}$ (meV Å)	$c_{\text{ex}}$ (meV Å)	$c_{\text{exp}}$ (meV Å)	$(\alpha + \beta)_{\text{exp}}$ (Å <sup>2</sup> )	$(\alpha + \beta)_{\text{calc}}$ (Å <sup>2</sup> )	$\alpha$ (Å <sup>2</sup> )	$\beta$ (Å <sup>2</sup> )
Li	44.58	29.00	36.5 ± 3.0	0.09 ± 0.04	-0.026	-0.447	0.4213
Na	19.51	10.35	18.5 ± 1.0	0.28 ± 0.04	0.212	-0.604	0.8163
K	12.56	4.13	15.5 ± 1.0	0.79 ± 0.11	0.741	-0.884	1.6247
Rb	7.17	0.45 <i>i</i>	9.2 ± 0.5	1.03 ± 0.11	0.985	-1.087	2.0721
Cs	5.30	1.57 <i>i</i>	7.5 ± 0.4	1.28 ± 0.14	1.362	-1.199	2.5619
Ca	24.05	15.06	28.5 ± 2.0	0.40 ± 0.08	0.516	-0.714	1.2295
Ba	10.43	5.54	18.8 ± 2.0	1.36 ± 0.16	1.187	-0.809	1.9957
Al	54.62	42.88	40.0 ± 4.0	-0.02 ± 0.03	0.254	-0.419	0.6730
Si	62.56	50.10	30.3 ± 3.0	-0.10 ± 0.01	0.277	-0.301	0.5785
Ge	35.01	27.37	20.5 ± 2.0	-0.07 ± 0.02	0.181	-0.406	0.5877
Ga	33.07	25.79	20.3 ± 2.0	-0.06 ± 0.02	0.045	-0.524	0.5690
Sn	24.44	18.46	19.0 ± 2.0	0.01 ± 0.04	0.221	-0.467	0.6877
Cd	18.84	13.77	14.2 ± 2.0	0.11 ± 0.06	0.109	-0.485	0.5939
Hg	17.49	13.22	13.8 ± 1.5	0.01 ± 0.04	-0.196	-0.467	0.2709
Pb	17.90	13.29	11.4 ± 1.0	-0.04 ± 0.02	0.068	-0.586	0.6543
Bi	18.24	13.53	13.1 ± 0.8	-0.01 ± 0.02	0.013	-0.672	0.6850

approximation is as follows [23]:

$$\delta_p = \frac{3}{2} + \frac{2}{15} \frac{U_{\text{ex}}}{Nk_B T}, \quad (18)$$

where  $N$  is the number of ions in the system and  $U_{\text{ex}}$  is the excess internal energy due to the ion-ion interaction. For pointlike ions,  $U_{\text{ex}}/N$  is given by

$$\frac{U_{\text{ex}}}{N} = \frac{(Z_i e)^2}{\pi} \int_0^\infty dq [S(q) - 1]. \quad (19)$$

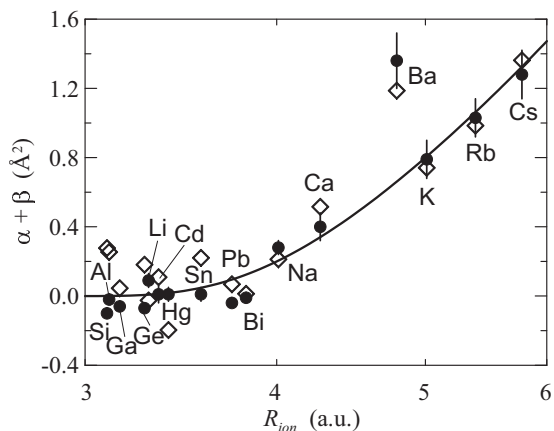


FIG. 4. Parameter  $\alpha + \beta$  as a function of the ion density parameter  $R_i$  (dots) in logarithm scale to expand the low-value region. Black dots are the data derived from the experiments (see text), while the lozenges are the present theoretical predictions. The thin lines are used to connect the element symbol to the corresponding dot when necessary. The full line is a guide to the eye plotted in order to make visible the dependence of  $\alpha + \beta$  on  $R_i$ .

It is worthwhile to mention that  $U_{\text{ex}}$  is almost always a negative quantity, the absolute value of which is much larger than the thermal energy  $Nk_B T$  when  $T$  is close to the melting point of all metals we analyzed. To calculate  $U_{\text{ex}}$ , we made use of the experimental static structure factors, which have been measured in all the systems here considered [28,34]. In principle, also in calculating  $U_{\text{ex}}$  one has to include an appropriate ion-ion interaction, however, we limit ourselves to the use of the above formulas because the extension to a real case is not straightforward.

To complete the calculation, one has to provide a reasonable estimate of  $\langle R^2 \rangle$ , which defines the shape of the ion-electron interaction as compared to that of pointlike ions. As a simple proposal, we derived  $\langle R^2 \rangle$  from the local pseudopotential as obtained by Harrison [26]. We preferred to resort to this old calculation which has the advantage of providing a *local* pseudopotential for all the systems of the present analysis. The quantity  $\langle R^2 \rangle$  is then calculated from the low  $q$  trend of the ion form factor  $F(q)$  tabulated in Ref. [26], since  $F(q) \simeq F(0)[1 - q^2 \langle R^2 \rangle / 6]$ . All these results are presented in Table II.

The general comparison between the theoretical estimates and the experimental result for  $2\delta_p/q_d^2 + \langle R^2 \rangle / 6$  is remarkably good considering the need for many approximations. The result is a quite convincing *experimental* evidence that  $\delta_p$  is negative in the strong coupling limit, since  $\langle R^2 \rangle$  is always a positive quantity and the small values for the sum  $2\delta_p/q_d^2 + \langle R^2 \rangle / 6$  cannot be obtained using a positively defined value for  $\delta_p$ . A negative value for  $\delta_p$  was expected from simulations [38], analytic approaches [23], and also in the homogeneous Bose gas [39]. It is very satisfactory that Fig. 4 provides an experimental support for the simulation and theoretical results for what concerns the negative value of  $\delta_p$ . We mention also that the results of Fig. 4 indicates that the experimental



determination of  $2\delta_p/q_d^2 + \langle R^2 \rangle/6$  shows a general trend as a function of the ion density with the specific characteristics of each ion giving only a minor contribution. A systematic trend of different elements as a function of  $r_s$  or  $Z_i$  was also considered in Ref. [14], although the dependence on  $R_i$  was not considered.

## VI. CONCLUSION

The first observation we can draw from the results reported in the previous section is that the proposed procedure provides a good estimate for the electron density useful to calculate the electron gas contribution to the collective mode velocity in a liquid metal. To perform in the best way the calculation, a proper procedure to determine the appropriate electron gas density has been introduced, which makes use of experimentally determined quantities, apart from the free-atom scattering factors  $f(Q)$ . In addition, we find that the two component model for a liquid metal is not confined to alkali metals, but it appears to be adequate also in liquid alkali-earth metals, polyvalent metals, and liquid semiconductors Si and Ge, which are metallic above the melting point. The model shows clearly the need for introducing all important features of the two components: the local field effects in the electron gas, which are adequately determined from the electron gas correlation energy, the  $q$  dependence of the plasma frequency  $\Omega(q)$  and the ion size effects in the ion-electron interaction potential. Looking at the trends emerging in Table II and Fig. 4, we notice that there is always a compensation between the two contributions  $\alpha$  and  $\beta$  and only in the case of alkali metals and alkali-earth metals a sizable total (positive) contribution is obtained. Interestingly, liquid Ba shows a rather large ( $\alpha + \beta$ ) contribution as determined from the experimental data, which is well reproduced by the present calculation. This compensation effect makes the quantitative calculation of the collective mode velocity more difficult because the relevant quantity ( $\alpha + \beta$ ) is rather small as compared to the values of  $\alpha$  and  $\beta$ . In any case, there is no straightforward interpretation for the compensation which is observed in the case of polyvalent metals. One can also observe that some minor discrepancy is present in the case of the metals having  $R_i \leq 4$ , an effect which appears to be maximum in Al, Sn, and Hg, but without any apparent trend.

It is also interesting to compare the present procedure to the approach of Ref. [22], which is basically a different version of the original two component model [2,3] extended to the whole  $Q$  range. Such an approach can be used to determine the collective mode velocity by taking the low-momentum limit in order to compare to the present results. In the calculation of Ref. [22], no special care has been devoted to the determination of the electron density parameter because it was applied to Na, Cu, Rb, and Au only and a rather straightforward choice was used. Within the description used in Ref. [22] the collective mode velocity is given by

$$c_{\text{ex}} = \frac{\Omega_p^2}{k_s^2} + \Omega_p^2 \frac{1}{4\pi^2 n^{(i)}} \times \int_0^\infty v_{\text{eff}}(Q) \left( -\frac{1}{15Q} \frac{dS}{dQ} - \frac{2}{5} \frac{d^2S}{dQ^2} \right) dQ, \quad (20)$$

where  $v_{\text{eff}}(Q)$  is an effective ion-electron potential, which is determined using a simple empiric approach. The screening wave vector was obtained using an interpolation scheme for the local field [40], which allows for an approximate evaluation of the dielectric function beyond the RPA. In the case of Na and Rb, the calculated velocities using this approach are 16.70 and 8.72 meV Å, respectively, to be compared with the present estimates 16.89 and 9.00 meV Å. These results show that there is a good agreement between the two procedures, that is both approximations contain the same relevant physics. We think that the advantage of the procedure we propose is in the possibility of determining the electron gas density and hence the ion charge without resorting to some assumption on the actual electron states. It is interesting to mention that a recent neutron scattering experiment on Au [41] provides a collective mode velocity of  $18.9 \pm 1.0$  meV Å =  $2870 \pm 150$  m/s, to be compared to  $15.98$  meV Å =  $2430$  m/s determined in Ref. [22]. We do not apply the present approach to Au because we do not consider the experimental  $S(Q)$  accurate enough, because of the oscillations that extend at high  $Q$ . There is no explanation for the observed disagreement with the results of Ref. [22], considering that the experiment is in good agreement with an *ab initio* simulation [41]. Probably the electron configuration used in the calculation is not adequate for this high- $Z$  element.

In liquid metals, it is also found that in the low momentum region the mode damping as determined by fitting the experimental dynamical structure factor with a damped harmonic oscillator is proportional to the mode frequency [14]. We recall also that in the case of Ga, it is found that on increasing the temperature from 320 to 970 K, the damping factor  $\Gamma(Q)$  does not increase [10]. A similar behavior is present also in the case of lithium ammonia solutions [12,13] where, on increasing the temperature from 220 to 250 K, again a small decrease from  $0.88 \pm 0.07$  to  $0.67 \pm 0.07$  of  $\Gamma(Q)$  is found. This observation indicates that the damping originates from a quasistatic effect related to the disordered structure, so that we can speculate that the *local quasistatic* density fluctuations contribute to  $\Gamma(Q)$  as it could be expected if one considers that

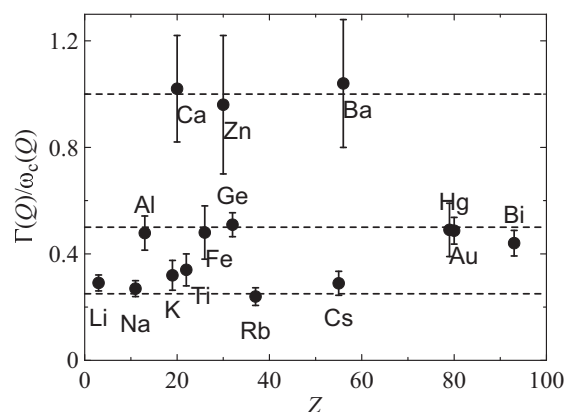


FIG. 5. Ratio of the damping parameter as measured by the nominal full width at half maximum and frequency of the collective modes as described by a damped harmonic oscillator in the low-momentum region (full dots) as a function of the atomic number. The dashed lines show the *magic numbers* 0.25, 0.50, and 1.00, which seem to correspond to the three groups of elements.

the ion-ion and ion-electron interaction are strongly screened by the electron gas. This view is similar to the structural relaxation discussed, for instance, in Ref. [42] where the collective modes are described in terms of an empiric memory function. The calculation of the local density fluctuations is not a simple task and it is beyond the primary concern of the present paper. Here, we simply report a qualitative trend, which is seen in Fig. 5, where the ratio of the damping factor  $\Gamma(Q)$  to the mode frequency  $\omega_c(Q)$  as a function of the atomic number is presented. The most striking result is the grouping of the  $\Gamma(Q)$  to  $\omega_c(Q)$  ratios close to the three *magic* values 0.25, 0.50, and 1.00, but no evident systematic trend along the periodic table or as a function of some specific characteristic of the element is visible. This result was already observed in Ref. [14]. Here we report some additional experimental results, namely, Ti [43], Fe [44], Zn [45], and Au [41], while the result for Bi is modified after taking the data at the lowest  $Q$  value available [33]. It is seen that the  $\Gamma(Q)$  to  $\omega_c(Q)$  ratio is close to 0.5 in the case of the early transition metal Ti, in the transition metal Fe, and in the nominally  $5d$  filled shell Au, while it is close to one in the case of Zn, which has a filled  $3d$  shell.

Finally, we observe that, in principle, the present procedure could be also tested in the case of metals having a more complex electronic structure, e.g., transition metals. Of course, in these last systems, the ion-electron potential has to be considered with some care and the possibility of applying the present approach is not straightforward because a nonlocal ion-electron potential could be necessary. Nonetheless, we used the present model also in this case, thanks to the available data [43,44] on the dynamics of liquid Ti and Fe, an early  $3d$  transition metal and a typical transition metal. We calculated the ion charges from Eq. (5) to derive the electronic contribution  $c_{\text{ex}}$  to the collective mode velocity.

Using the experimental structure factor [46,47] of liquid Ti and Fe, we find an interstitial electron density parameter  $r_s = 2.242$  for Ti and  $r_s = 1.947$  for Fe, corresponding to ion charges equal to 2.65 and 2.87, respectively. Interestingly, the ion charges as determined using the crystal approximation of Eq. (10) are 2.65 and 2.75, respectively, for Ti and Fe and for

both fcc and bcc structures. The difference between the liquid and the crystal approximation suggests that the actual liquid structure is fairly complex as it has been suggested in the case of iron [47]. In any case, the interstitial electron density in Ti and Fe suggests that  $3d$  electrons give a minor contribution to the electronic density in the case of Ti and Fe. Using these electron densities, we find  $c_{\text{RPA}} = 39.07 \text{ meV \AA}$  and  $c_{\text{ex}} = 30.50 \text{ meV \AA}$  in the case of Ti and  $c_{\text{RPA}} = 43.34 \text{ meV \AA}$  and  $c_{\text{ex}} = 35.28 \text{ meV \AA}$  in the case of Fe. These results should be compared with the experimental results [43,44]  $c_{\text{exp}} = 29.7 \pm 3.0 \text{ meV \AA}$  and  $c_{\text{exp}} = 28.4 \pm 2.0 \text{ meV \AA}$  for Ti and Fe, respectively. Therefore  $(\alpha + \beta)_{\text{exp}} = -0.01 \pm 0.03 \text{ \AA}^2$  in Ti and  $(\alpha + \beta)_{\text{exp}} = -0.05 \pm 0.01 \text{ \AA}^2$  in Fe. These data suggest that meaningful results can be obtained also in these transition metals and there is still an almost full compensation of the two ionic contributions even in the case of Ti and Fe, where more complex ion-ion and ion-electron interactions are expected. In addition, we observe also that the damping in Fe appears in the same group of the polyvalent metals indicating that, contrary to the case of alkali metals, the ion charge higher than one plays some role. It is also interesting to mention that while the  $\Gamma(Q)$  to  $\omega_c(Q)$  ratio of Fe is close to that of polyvalent metals Al, Ge, Hg, and Bi, this ratio in the case of Ti is closer to that of the alkali metals. On the other hand,  $\Gamma(Q)/\omega_c(Q)$  of Zn is close to that of Ca and Ba, which have the same nominal valence. To show that some correlation between the ion charge and the ratio  $\Gamma(Q)/\omega_c(Q)$  exists, we observe that the average ion charge of the alkali metals is equal to 1.00, that of the metals Al, Fe, Ge, Hg, and Bi is 2.97 and that of Ca and Ba is 1.84, while  $Z_i$  of Zn is calculated to be 2.99, so that  $\Gamma(Q)/\omega_c(Q)$  has some dependence on  $Z_i$  but Ti and Zn do not follow this behavior. Nonetheless, considering that  $\Gamma(Q)/\omega_c(Q)$  probably depends on the electron density fluctuations, a straightforward relationship with  $Z_i$  is not expected as some dependence on the actual structure is expected. Further work is necessary to calculate the electron density fluctuations and to identify a quantitative correlation between them and the ratio  $\Gamma(Q)/\omega_c(Q)$ .

- 
- [1] D. Pines, *Elementary Excitations in Solids* (Benjamin, New York, 1963).
- [2] N. H. March, *Liquid Metals* (Cambridge University Press, Cambridge, 1990).
- [3] J. Bardeen and D. Pines, *Phys. Rev.* **99**, 1140 (1955).
- [4] J. P. Hansen and I. R. McDonald, *Theory of Simple Liquids*, 2nd ed. (Academic Press, London, 1986).
- [5] Y. R. Wang and A. W. Overhauser, *Phys. Rev. B* **35**, 501 (1987).
- [6] F. Postogna and M. P. Tosi, *Nuovo Cim. B* **55**, 399 (1980).
- [7] D. K. Chaturvedi, M. Rovere, G. Senatore, and D. Pines, *Physica B* **111**, 11 (1981).
- [8] L. E. Bove, F. Sacchetti, C. Petrillo, and B. Dorner, *Phys. Rev. Lett.* **85**, 5352 (2000).
- [9] L. E. Bove, B. Dorner, C. Petrillo, F. Sacchetti, and J.-B. Suck, *Phys. Rev. B* **68**, 024208 (2003), and references therein.
- [10] L. E. Bove, F. Formisano, F. Sacchetti, C. Petrillo, A. Ivanov, B. Dorner, and F. Barocchi, *Phys. Rev. B* **71**, 014207 (2005).
- [11] C. A. Burns, P. M. Platzman, H. Sinn, A. Alatas, and E. E. Alp, *Phys. Rev. Lett.* **86**, 2357 (2001).
- [12] F. Sacchetti, E. Guarini, C. Petrillo, L. E. Bove, B. Dorner, F. Demmel, and F. Barocchi, *Phys. Rev. B* **67**, 014207 (2003).
- [13] C. Petrillo, F. Sacchetti, E. Guarini, L. E. Bove, and F. Demmel, *Phys. Rev. B* **84**, 094206 (2011).
- [14] L. E. Bove, C. Petrillo, and F. Sacchetti, *Cond. Matt. Phys.* **11**, 119 (2008).
- [15] V. L. Moruzzi, J. F. Janak, and A. R. Williams, *Calculated Electronics Properties of Metals* (Pergamon, New York, 1978).
- [16] L. Hedin and B. I. Lundqvist, *J. Phys. C* **4**, 2064 (1971).
- [17] M. M. Sigalas, J. H. Rose, D. A. Papaconstantopoulos, and Herbert B. Shore, *Phys. Rev. B* **58**, 13438 (1998).
- [18] J. P. Perdew, F. Nogueira, and C. Fiolhais, *J. Mol. Struct. (Theochem)* **501–502**, 271 (2000).
- [19] S. Baroni, S. de Gironcoli, A. Dal Corso, and P. Giannozzi, *Rev. Mod. Phys.* **73**, 515 (2001), and references therein.

- [20] A. A. Louis and N. W. Ashcroft, *Phys. Rev. Lett.* **81**, 4456 (1998).
- [21] Y. R. Wang and A. W. Overhauser, *Phys. Rev. B* **35**, 497 (1987).
- [22] Y. R. Wang and A. W. Overhauser, *Phys. Rev. B* **38**, 9601 (1988).
- [23] S. Ichimaru, *Rev. Mod. Phys.* **54**, 1017 (1982).
- [24] C. F. Richardson and N. W. Ashcroft, *Phys. Rev. B* **50**, 8170 (1994).
- [25] C. Petrillo, F. Sacchetti, and G. Mazzone, *Acta Crystallogr. A* **54**, 468 (1998).
- [26] W. E. Harrison, *Pseudopotentials in the Theory of Metals* (W. A. Benjamin, New York, 1966), p. 310.
- [27] J. H. Hubbell and I. Øverbø, *J. Phys. Chem. Ref. Data* **8**, 69 (1979).
- [28] U. Dalborg and L. G. Olsson, *J. Phys. F* **13**, 555 (1983).
- [29] C. Kittel, *Quantum Theory of Solids*, 2nd ed. (Wiley, New York, 1987).
- [30] P. Gori-Giorgi, F. Sacchetti, and G. B. Bachelet, *Phys. Rev. B* **61**, 7353 (2000).
- [31] G. G. Spink, R. J. Needs, and N. D. Drummond, *Phys. Rev. B* **88**, 085121 (2013).
- [32] J. R. D. Copley and J. M. Rowe, *Phys. Rev. Lett.* **32**, 49 (1974); T. Scopigno, U. Balucani, G. Ruocco, and F. Sette, *Phys. Rev. E* **63**, 011210 (2000); C. Morkel and T. Bodensteiner, *J. Phys.: Condens. Matter* **2**, 251 (1990); S. Hosokawa, Y. Kawakita, W.-C. Pilgrim, and H. Sinn, *Phys. Rev. B* **63**, 134205 (2001); T. Scopigno, U. Balucani, G. Ruocco, and F. Sette, *Phys. Rev. E* **65**, 031205 (2002); S. Hosokawa, J. Greif, F. Demmel, and W.-C. Pilgrim, *Chem. Phys.* **292**, 253 (2003); F. Sacchetti, L. E. Bove, E. Guarini, A. Orecchini, L. Sani, and C. Petrillo (unpublished); F. Formisano, E. Guarini, C. Petrillo, and F. Sacchetti (unpublished); O. Soderstrom, J. R. D. Copley, J.-B. Suck, and B. Dorner, *J. Phys. F: Met. Phys.* **10**, L151 (1980).
- [33] L. Sani, L. E. Bove, C. Petrillo, and F. Sacchetti, *J. Non-Cryst. Solids* **353**, 3139 (2007).
- [34] W. van der Lugt and B. P. Alblas, *Handbook of Thermodynamic and Transport Properties of Alkali Metals*, edited by R. W. Ohse (Blackwell, Oxford, 1985); Y. Waseda, *The Structure of Non-Crystalline Materials - Liquid and Amorphous Solids*, (McGraw-Hill, New York, 1980); J. M. Stallard and C. M. Davis, *Phys. Rev. A* **8**, 368 (1973); J. P. Gabathuler and S. Steeb, *Z. Naturforsch.* **34A**, 1314 (1979); A. Bizid, L. Bosio, and R. Cortes, *J. Chim. Phys. Phys. Chim. Biol.* **74**, 863 (1977); M. K. Gardiner, P. Colbourne, and C. Norris, *Philos. Mag.* **B 54**, 133 (1986).
- [35] S. A. Serebrinsky, J. L. Gervasoni, J. P. Ariata, and V. H. Ponce, *J. Mat. Sci.* **33**, 167 (1998).
- [36] D. A. Papaconstantopoulos, *Handbook of the Band Structure of Elemental Solids* (Plenum Press, New York, 1986), p 205.
- [37] P. M. Raccach and V. E. Henrich, *Phys. Rev.* **184**, 607 (1969).
- [38] J. P. Hansen, E. L. Pollock, and I. R. McDonald, *Phys. Rev. Lett.* **32**, 277 (1974).
- [39] H. M. Böhm, S. Conti, and M. P. Tosi, *J. Phys.: Condens. Matter* **8**, 781 (1996).
- [40] Y. R. Wang, M. Ashraf, and A. W. Overhauser, *Phys. Rev. B* **30**, 5580 (1984).
- [41] E. Guarini, U. Bafile, F. Barocchi, A. De Francesco, E. Farhi, F. Formisano, A. Laloni, A. Orecchini, A. Polidori, M. Puglini, and F. Sacchetti, *Phys. Rev. B* **88**, 104201 (2013).
- [42] T. Scopigno, G. Ruocco, and F. Sette, *Rev. Mod. Phys.* **77**, 881 (2005); T. Scopigno, U. Balucani, G. Ruocco, and F. Sette, *J. Phys.: Condens. Matter* **12**, 8009 (2000).
- [43] A. H. Said, H. Sinn, A. Alatas, C. A. Burns, D. L. Price, M. L. Saboungi, and W. Schirmacher, *Phys. Rev. B* **74**, 172202 (2006).
- [44] S. Hosokawa, M. Inui, K. Matsuda, D. Ishikawa, and A. Q. R. Baron, *Phys. Rev. B* **77**, 174203 (2008).
- [45] L. Sani, A. Orecchini, A. Paciaroni, E. Guarini, C. Petrillo, and F. Sacchetti (unpublished).
- [46] G. W. Lee, A. K. Gangopadhyay, K. F. Kelton, R. W. Hyers, T. J. Rathz, J. R. Rogers, and D. S. Robinson, *Phys. Rev. Lett.* **93**, 037802 (2004).
- [47] T. Schenk, D. Holland-Moritz, V. Simonet, R. Bellissent, and D. M. Herlach, *Phys. Rev. Lett.* **89**, 075507 (2002).